Coupled Oscillators

DOI: 10.1002/anie.201201962

Pulse-Coupled Chemical Oscillators with Time Delay**

*Viktor Horvath, Pier Luigi Gentili, Vladimir K. Vanag, and Irving R. Epstein**

Cooperative behavior of biological oscillators, including networks of neurons,[1] can be mimicked and may be studied using simpler systems composed of coupled chemical oscillators. Chemical oscillators are typically coupled through continuous mass exchange[2] or electrochemical linkage.[3] The interactions between them may take place instantaneously or with a time delay[4] and may be global or local.[5] Coupling can be unidirectional or reciprocal. The term "diffusive coupling" is often employed to refer to local reciprocal coupling by mutual mass exchange.

In chemical systems, excitatory diffusive coupling, realized by mass exchange of an activator, leads to in-phase synchronization of oscillators, whereas inhibitory diffusive coupling, implemented by mass exchange of an inhibitor, results in anti-phase oscillations.[6]

Diffusive coupling differs fundamentally, however, from the interaction between neurons. Neurotransmission is typically unidirectional and takes place by discrete pulses of neurotransmitters at synapses, without continuous mass exchange. Therefore, analysis of pulse-coupled oscillators[1,7] has received considerable attention. Theoretical studies demonstrate that introduction of a time delay between a trigger event and the resulting pulse may result in counter-intuitive behavior,[8] for example, in-phase synchronization in inhibitory pulse-coupled systems and out-of-phase oscillations with excitatory coupling. These behaviors have not yet been observed in coupled chemical oscillators.

Herein, we investigate the dynamics of a pair of pulse-coupled ferroin-catalyzed Belousov–Zhabotinsky (BZ)[9] oscillators with time delay operated in continuously fed stirred tank reactors (CSTRs). The activator in the BZ reaction is $HBrO_2$, while the inhibitor is Br^-, which plays the key role in controlling oscillations.[10] Therefore the most effective method of coupling is controlling the concentration of Br^- ions in one oscillator through a signal from the other.

An increase in $[Br^-]$ is realized in our experiments by addition of a small volume of KBr solution from an external source (reservoir). If this injection is controlled by the other oscillator, we have inhibitory coupling. By decreasing $[Br^-]$, the system can be activated. In experiments with excitatory coupling, we used a solution of $AgNO_3$ from an external reservoir to lower $[Br^-]$ through formation of AgBr precipitate.[11] We investigated symmetric, reciprocal, inhibitory, and excitatory coupling, as well as mixed coupling, where oscillator 1 is inhibited by oscillator 2 and oscillator 2 is activated by oscillator 1.

To simulate our experimental results, we constructed a five-variable model of the BZ reaction, which is described in the Supporting Information.

In experiments with mutual inhibitory coupling, both reservoirs contained the same solution of inhibitor, and coupling was symmetric, with the same discharged volumes and time delays for both oscillators. The dynamics of the system were observed at several sets of concentrations of BZ reactants and CSTR residence times, k_0^{-1}. We found four dynamic behaviors, shown in Figure 1 a–d. In all experiments, the time delay, τ, was less than half the period of the uncoupled oscillators.

At relatively small time delay and $[KBr]_{inj}$, we observed anti-phase (AP) oscillations (Figure 1 a). At larger τ and $[KBr]_{inj}$, a transition from AP to IP oscillations occurred (Figure 1 b). At even higher $[KBr]_{inj}$ without time delay, we found complex oscillations (Figure 1 c), where the numbers of spikes in the two CSTRs differed, and the oscillations were irregular. Finally, at very strong coupling, one oscillator was suppressed, while the other oscillated at its natural frequency (OS regime), since the suppressed oscillator was unable to affect the counter-oscillator (Figure 1 d). The OS regime is an example of symmetry-breaking of two identical coupled oscillators resulting in unidirectional coupling.

The results of the corresponding simulations are shown in Figure 1 e–k. Note that the simulated dynamics are presented by plotting variables z_1 and z_2, the concentrations of oxidized catalyst in the two oscillators, versus time, while in the experimental results, the plotted signal is a mixed potential measured by a platinum versus reference (Ag | AgCl | KCl) electrode pair, which depends logarithmically on the concentrations of several species. Three examples of complex oscillations (C-domain in panel (e) of Figure 1) are presented in panels (h–j). Panel (h) demonstrates period doubling (purple squares in (e)). Panel (i) shows typical irregular oscillations, where the numbers of spikes in the two oscillators differ. Panel (j) illustrates regular complex oscillations, in

[*] Prof. V. Horvath, Prof. P. L. Gentili, Prof. V. K. Vanag, Prof. I. R. Epstein
Department of Chemistry, Brandeis University
Waltham, MA 02454-9110 (USA)
E-mail: epstein@brandeis.edu
Prof. V. Horvath
Institute of Chemistry, Department of Analytical Chemistry, L. Eötvös University
P.O. Box 32, 1518 Budapest (Hungary)
Prof. P. L. Gentili
Department of Chemistry, University of Perugia
06123 Perugia (Italy)
Prof. V. K. Vanag
Immanuel Kant Baltic Federal University
A. Nevskogo 14, Kaliningrad, 236041 (Russia)

[**] This work was supported by the National Science Foundation (grant CHE-1012428 and MRSEC grant DMR-0820492), the Army Research Office (grant W91NF-49-0496), and the Hungarian Academy of Sciences (grants OTKA 67701 and 100891).

Supporting information for this article is available on the WWW under http://dx.doi.org/10.1002/anie.201201962.

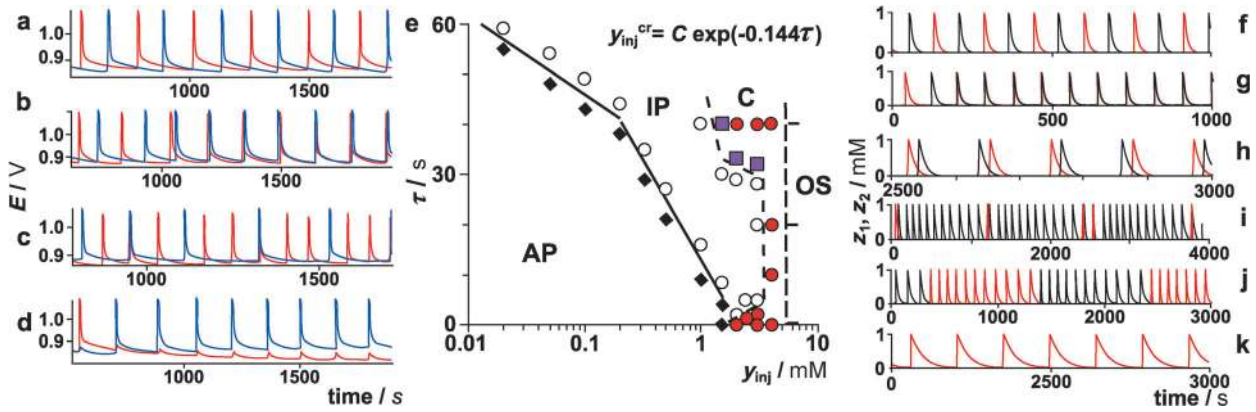

Figure 1. Inhibitory pulse-coupled BZ oscillators. The two oscillators are shown in different colors. a–d) Experiment, traces of Pt electrodes; e–k) simulations. a) and f) anti-phase (AP) oscillations (diamonds in (e)); b) and g) in-phase (IP) oscillations (open circles in (e)); c) and h–j) complex (C) oscillations (red circles in (e)); d) and k) OS regime; h) period doubling (squares in C-domain in (e)). Experimental parameters: a) $[KBr]_{inj} = 0.0431$ mM, $\tau = 0$; $T_{AP} = 250$ s. (T = period; $[KBr]_{inj} = V_{inj}[KBr]_S/V_0$, where V_{inj} is the volume of bromide injected from the reservoir, where its concentration is $[KBr]_S$) b) Initially AP oscillations at $[KBr]_{inj} = 0.053$ mM and $\tau = 0$ s switch to IP at the same $[KBr]_{inj}$ and $\tau = 20$ s; $T_{IP} = 150$ s. c) $[KBr]_{inj} = 0.517$ mM, $\tau = 0$ s. d) $[KBr]_{inj} = 1.08$ mM, $\tau = 0$ s; $T = 140$ s. Initial concentrations of reactants in CSTRs are $[NaBrO_3]_0 = 0.25$ M, $[MA]_0 = 0.05$ M (a,b,d), 0.5 M (c), $[H_2SO_4]_0 = 0.2$ M (a,b,d), 0.3 M (c), and $[ferroin]_0 = 1$ mM (MA = malonic acid). Residence time, $k_0^{-1} = 1832$ s (a,b,d), 1200 s (c). Coupling strength, γ_{inj} [mM], and time delay, τ [s] are f) 1.5, 0, g) 1.5, 5, h) 1.5, 40, i) 4, 40, j) 4, 0, k) 6, 0, respectively.

which groups of oscillations containing equal numbers of spikes alternate with suppressed periods.

For mutual excitatory coupling, the coupling parameters were again identical for both oscillators, but KBr was replaced by $AgNO_3$ in both reservoirs. Varying the time delay and the coupling strength, $[AgNO_3]_{inj}$, we found five main behaviors, shown in Figure 2 a–e. At small coupling strength and τ, we observed almost in-phase (AIP) oscillations (Figure 2 a). When a spike occurred in CSTR-1 (blue trace in Figure 2 a), a pulse of $AgNO_3$ was injected into CSTR-2 (red trace in Figure 2 a), inducing autocatalysis. However, the small feedback pulse triggered by CSTR-2 cannot generate a new spike in CSTR-1 owing to the refractory period that comes after a spike. The phase shift between two AIP oscillations is equal to τ plus the time needed for the autocatalysis to start. AIP oscillations constitute another example of symmetry-breaking of two identical coupled oscillators.

When we increased $[AgNO_3]_{inj}$ above a threshold, comparable to $[Br^-]$ during the refractory period, we observed bursting behavior at smaller τ (Figure 2 b). The period of the fast AP oscillations in the bursts was greater than 2τ, again because of the time necessary for autocatalysis to start. At slightly different coupling strengths, several bursting regimes with different numbers of spikes per burst were observed. At very small τ (less than a few seconds) bursting patterns cannot be observed, because the immediate addition of $AgNO_3$ does not generate a new spike. At larger τ, regular fast AP oscillations (FAP) with period slightly larger than 2τ were

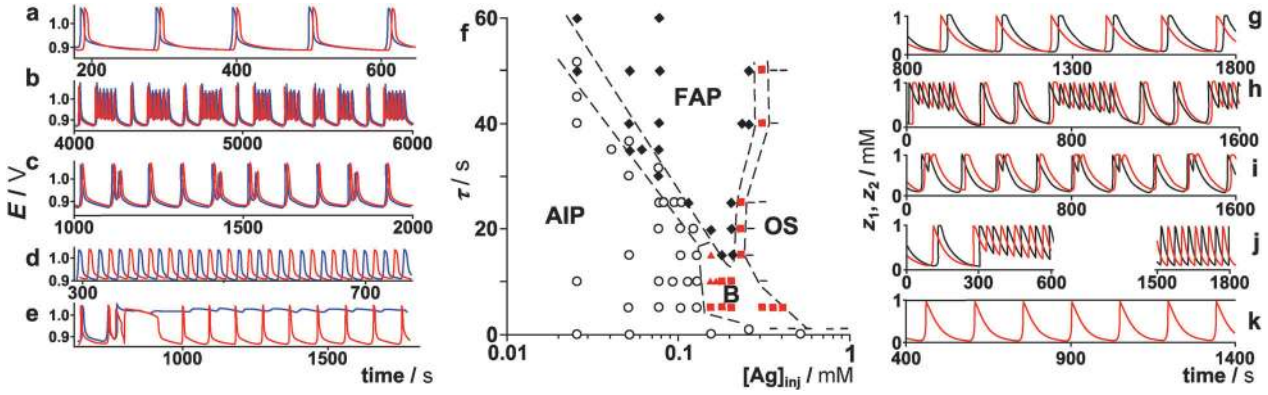

Figure 2. Excitatory pulse-coupled BZ oscillators. a–e) Experiment, traces of Pt-electrodes; g–k) simulations. a) $[AgNO_3]_{inj} = 0.0138$ mM, $\tau = 0$, $T = 107$ s; b) $[AgNO_3]_{inj} = 0.0405$ mM, $\tau = 5$ s. Period of fast AP oscillations in bursts is approximately 21 s. c) $[AgNO_3]_{inj} = 0.0378$ mM, $\tau = 4$ s; d) $[AgNO_3]_{inj} = 0.0405$ mM, $\tau = 10$ s; $T = 28$ s. e) $[AgNO_3]_{inj} = 3.78$ mM, $\tau = 35$ s. Initial concentrations of reactants in CSTRs are $[NaBrO_3]_0 = 0.25$ M, $[MA]_0 = 0.05$ M, $[H_2SO_4]_0 = 0.2$ M, and $[ferroin]_0 = 1$ mM, $k_0^{-1} = 1832$ s (a), 659 s (b–e). Coupling strength $[Ag]_{inj}$ [mM] and time delay τ [s] are: g) 0.103, 20; h) 0.155, 15; i) 0.18, 10; j) 0.128, 20; k) 0.927, 0. Symbols in (f): AIP (open circles), corresponding to panel (g); FAP (black diamonds),second part of (j); B (red triangles and squares), bursting, triangles for irregular bursts as in (h) and squares for short bursts as in (i); OS (–), as in (k).

found (Figure 2d). After several tens of fast oscillations, the FAP oscillations lost stability because of the dilution of the reaction mixture caused by the repetitive injection of activator solution. Once the original concentrations were restored by the inflow of the BZ reactants, the FAP oscillations resumed.

At very large $[AgNO_3]_{inj}$, we observed an OS regime (Figure 2e), but with the suppressed oscillator in the oxidized state. Between the FAP and OS regimes, we found a regime of short bursts consisting of two spikes, which alternated (usually irregularly) with almost in-phase single oscillations (Figure 2c).

Computational results are presented in Figure 2 f–k.

In experiments with mixed excitatory-inhibitory pulse-coupling, one oscillator was perturbed by the activator ($AgNO_3$) and the other by the inhibitor (KBr). Typical patterns at $\tau = 25$ s are shown in Figure 3a–e). The 1:1 resonance (Figure 3, panel (a)) at small $[KBr]_{inj}$ is similar to AIP oscillations. The phase shift between the oscillators is almost equal to τ. We found other m:n resonances at higher $[KBr]_{inj}$ or different $[AgNO_3]_{inj}$. Examples of 4:5, 1:2, 1:3 resonances and an OS regime (with the suppressed oscillator in the reduced state) are presented in Figure 3 panels b, c, d, and e, respectively. All these resonances emerge because injection of the inhibitor extends the oscillation period, while the activator has the opposite effect.

Selected results of simulations are presented in Figure 3 f–m. All resonances found in the experiments are reproducible with our model. The boundary between 1:1 and other m:n resonances may have either positive slope, $d[Ag]_{inj}/dy_{inj}$, (as in Figure 3 panel f at $\tau = 25$ s) or negative slope (at $\tau = 0$ s, shown in Figure S3 in the Supplementary Materials).

In addition to the anticipated IP and AP oscillations for both inhibitory and excitatory pulse coupling, we have found several other modes, such as FAP, OS, bursting, complex oscillations, and m:n resonances. In general, all boundaries between these modes (in the y_{inj}–τ, $[Ag]_{inj}$–τ, and y_{inj}–$[Ag]_{inj}$ parametric planes) can be described and understood with our model. As an example, we analyze in the Supporting Information the transition between the AP and IP domains in Figure 1e.

We have demonstrated that pulse coupling with time delay in two BZ oscillators leads to new dynamic behaviors. Our experimental method of introducing a purely inhibitory or excitatory coupling may be implemented in other coupled chemical oscillators, for example, pH oscillators,[12] where an acid/base pair can serve as the activator/inhibitor. This novel method of coupling allows us to conduct experiments where mode-dependent coupling is realized (coupling occurs only in the oscillatory and not in the steady-state mode), and the coupling strength and the time delay are variables, which may be useful for future chemical computers. Time delay has been shown to be important for the robustness of neuron networks.[13] Pulse-coupling, unlike diffusive coupling, 1) is a highly nonlinear process that can lead to complicated behavior of the coupled oscillators, and 2) couples oscillators through their excited state, in contrast to coupling through a steady state, as in Turing or wave instability.[14] It can therefore lead to previously unseen patterns.

Experimental Section

Deionized water and the following analytical grade chemicals were used to prepare solutions without further purification: $NaBrO_3$ (99+%, Acros Chemicals), tris-(1,10-phenantroline)iron(II) solution (0.025 M, Ricca Chemical Company), malonic acid (MA) (99%, Acros Chemicals), H_2SO_4 (10N, Fisher), KBr (99+%, Janssen Chimica), $AgNO_3$ (100%, Fisher), $HClO_4$ (70%, Fisher), K_2SO_4 (99+%, Acros Chemicals).

Our arrangement for synapse-like pulse-coupling is shown schematically in Figure S1 of the Supporting Information, where

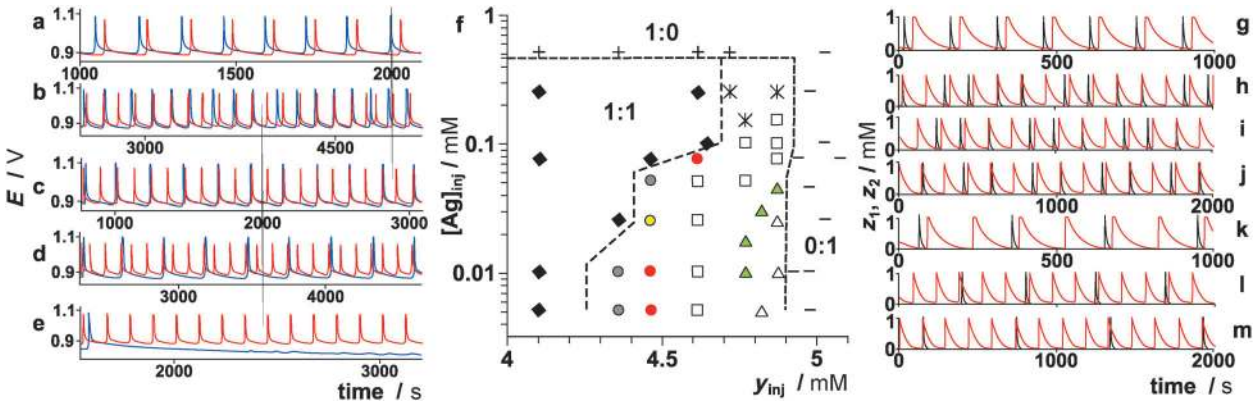

Figure 3. Mixed excitatory–inhibitory coupling. a–e) Representative examples of experimental resonances n:m for two excitatory–inhibitory pulse-coupled BZ oscillators with time delay $\tau = 25$ s. Inhibitor (KBr) is pulse-injected into CSTR-1 (blue curves) and activator ($AgNO_3$) into CSTR-2 (red curves). The ratios of the numbers of spikes per global period are a) 1:1; b) 4:5; c) 1:2; d) 1:3, and e) 0:1. The initial concentrations of reactants in the CSTRs are the same as in Figure 1. Pulse-injected concentrations of inhibitor and activator, respectively, are (in mM) a) 0.01 and 0.0069, b) 0.01 and 0.01, c) 0.048 and 0.0069, d) 0.048 and 0.0014, and e) 0.1 and 0.0069. f–m) Simulations for $\tau = 25$ s. Coupling strengths, γ_{inj} and $[Ag]_{inj}$, respectively, (mM): g) 1:1, 4.1, 0.077; h) 4:5, 4.46, 0.0513; i) 3:4, 4.46, 0.0257; j) 2:3, 4.46, 0.00513; k) 1:2, 4.62, 0.0103; l) 1:3, 4.77, 0.0103; m) 1:4, 4.87, 0.0257. In (f) black diamonds 1:1; gray circles $1 > n/m > 0.75$; yellow circles 3:4; red circles 2:3; open squares 1:2; green triangles 1:3; open triangles 1:4; stars irregular oscillations, $0.5 > n/m > 0.33$; + 1:0 (the oscillator receiving activator is suppressed); − 0:1 (the oscillator receiving inhibitor is suppressed).

additional details are given. Herein we explain only the main idea of the experiments. The BZ oscillations in the CSTRs are monitored by Pt electrodes. A high amplitude spike in the redox potential of one oscillator triggers a pulse discharge of a small volume of solution of either activator or inhibitor from reservoir A or B into the other CSTR by a computer-controlled solenoid valve. These injections play a role analogous to the release of neurotransmitters in synapses. The amount of discharged solution depends linearly on the duration of the open state of the valve, t_v, since the flow rates from the reservoirs are kept constant. Therefore we control the coupling strength (which is proportional to the injected concentration of either inhibitor or activator) through t_v. The time delay, τ, between the trigger event (occurrence of a spike) and the opening of the valve is also set by the computer program. This time is analogous to the delay in neurotransmitter release due to time needed for signal transduction.

Received: March 12, 2012
Published online: June 5, 2012

Keywords: Belousov–Zhabotinsky Reaction · coupled oscillators · neuron networks · pulse coupling · time delay

[1] M. I. Rabinovich et al., *Rev. Mod. Phys.* **2006**, *78*, 1213 – 1265.
[2] I. R. Epstein, K. Showalter, *J. Phys. Chem.* **1996**, *100*, 13132 – 13147.
[3] a) W. Hohmann, M. Kraus, F. W. Schneider, *J. Phys. Chem. A* **1999**, *103*, 7606 – 7611; b) M. F. Crowley, R. J. Field, *J. Phys. Chem.* **1986**, *90*, 1907 – 1915.
[4] a) D. Goldobin, M. Rosenblum, A. Pikovsky, *Phys. Rev. E* **2003**, *67*, 061119; b) R. Holz, F. W. Schneider, *J. Phys. Chem.* **1993**, *97*, 12239 – 12243.
[5] a) J. A. Acebrón et al., *Rev. Mod. Phys.* **2005**, *77*, 137 – 185; b) I. Z. Kiss, Y. Zhai, J. L. Hudson, *Science* **2002**, *296*, 1676 – 1678.
[6] M. Toiya, V. K. Vanag, I. R. Epstein, *Angew. Chem.* **2008**, *120*, 7867 – 7869; *Angew. Chem. Int. Ed.* **2008**, *47*, 7753 – 7755.
[7] a) P. Ashwin, M. Timme, *Nonlinearity* **2005**, *18*, 2035 – 2060; b) V. V. Klinshov, V. I. Nekorkin, *Chaos Solitons Fractals* **2011**, *44*, 98 – 107; c) C. Ly, G. B. Ermentrout, *SIAM J. Appl. Dynam. Sys.* **2010**, *9*, 113 – 137; d) A. Rothkegel, K. Lehnertz, *EPL* **2011**, *95*, 38001; e) W. Wu, B. Liu, T. P. Chen, *Neural Networks* **2010**, *23*, 783 – 788.
[8] a) M. Bartos, I. Vida, P. Jonas, *Nat. Rev. Neurosci.* **2007**, *8*, 45 – 56; b) U. Ernst, K. Pawelzik, T. Geisel, *Phys. Rev. Lett.* **1995**, *74*, 1570 – 1573; c) U. Ernst, K. Pawelzik, T. Geisel, *Phys. Rev. E* **1998**, *57*, 2150 – 2162; d) C. van Vreeswijk, L. F. Abbott, G. B. Ermentrout, *J. Comput. Neurosci.* **1994**, *1*, 313 – 321.
[9] a) B. P. Belousov, *Collection of Short Papers on Radiation Medicine*, Medgiz, Moscow, **1959**, pp. 145 – 152; b) A. M. Zhabotinsky, *Dokl. Akad. Nauk SSSR* **1964**, *157*, 392 – 395.
[10] R. J. Field, R. M. Noyes, *J. Chem. Phys.* **1974**, *60*, 1877 – 1884.
[11] a) J. Kosek, M. Marek, *J. Phys. Chem.* **1993**, *97*, 120 – 127; b) Z. Noszticzius, *J. Am. Chem. Soc.* **1979**, *101*, 3660 – 3663; c) P. Ruoff, J. Vestvik, *J. Phys. Chem.* **1989**, *93*, 7798 – 7801.
[12] O. Pešek, L. Schreiberová, I. Schreiber, *Phys. Chem. Chem. Phys.* **2011**, *13*, 9849 – 9856.
[13] V. P. Zhigulin et al., *Phys. Rev. E* **2003**, *67*, 021901.
[14] A. M. Turing, *Philos. Trans. R. Soc. London Ser. B* **1952**, *237*, 37 – 72.

